

Graphene superlattice with periodically modulated Dirac gap

G.M. Maksimova, E.S. Azarova, A.V. Telezhnikov, and V.A. Burdov

*Department of Physics, University of Nizhny Novgorod,
23 Gagarin Avenue, 603950 Nizhny Novgorod, Russian Federation*

(Dated: August 14, 2012)

Graphene-based superlattice (SL) formed by a periodic gap modulation is studied theoretically using a Dirac-type Hamiltonian. Analyzing the dispersion relation we have found that new Dirac points arise in the electronic spectrum under certain conditions. As a result, the gap between conduction and valence minibands disappears. The expressions for the position of these Dirac points in \mathbf{k} -space and threshold value of the potential for their emergence were obtained. At some parameters of the system, we have revealed interface states which form the top of the valence miniband.

PACS numbers: 71.10.Pm, 73.21.-b, 81.05.U-

I. INTRODUCTION

During for the last years extremely much attention was paid to the electronic properties of graphene (see Ref.1 for the review). Such interest results, in particular, from the fact that physics of the low-energy carriers in graphene is governed by a Dirac-type Hamiltonian. The band structure of an ideal graphene sheet has no energy gap. As a consequence, Dirac electrons become massless, and reveal unusual properties such as perfect transmission at normal incidence through any potential barrier (the Klein paradox^{2,3}), trembling motion (or Zitterbewegung⁴), etc. Because of the Klein effect, an electrostatic potential cannot confine electrons in graphene. This makes difficult to use graphene in electronic devices.⁵ To overcome this problem, one needs to create a gap in graphene. Another possible way for confining Dirac fermions is the use of spatially inhomogeneous magnetic field.⁶ The gap can be induced by substrate or strain engineering as well as by deposition or adsorption of molecules on a graphene layer. For example, two carbon sublattices of graphene placed on top of hexagonal boron nitride (*h*-BN) become nonequivalent due to their interaction with the substrate. The band-structure calculations within the local-density approximation for this system gives a gap not less than 53 meV.⁷ A hydrogenated sheet of graphene (graphane) is a semiconductor with a gap of the order of a few eV.⁸

Besides, it is possible to modulate spatially the gap (i.e. the particle's mass) in graphene. It was shown that the spatial mass dependence leads to suppression of Klein tunneling and induces confined states.^{9,10} The required gap modulation can be created, for instance, in graphene placed on a substrate fabricated from different dielectrics. It is also possible to use for this purpose an inhomogeneously hydrogenated graphene or graphene sheet with nonuniformly deposited CrO₃ molecules.

Correspondingly, one can fabricate different graphene heterostructures with the gap discontinuity. In particular, graphene-based superlattice (SL) can be formed due to the periodic modulation of the band gap. The model of such a superlattice has been proposed and discussed earlier.¹¹

In our work we analyze the electronic states in graphene-based SL with periodically modulated gap and relative band shift (potential). We consider the simplest case where the gap and potential are piecewise constant functions, and compute the SL band structure at various relationships between the gap and band shift. We have found in the SL spectrum new Dirac points whose positions in \mathbf{k} -space were determined. We also show that interface states can arise in the gap-induced SL. For this case the relevant conditions and system parameters were obtained.

II. DIRAC PARTICLE IN GRAPHENE SUPERLATTICE

Let us consider one-dimensional (1D) graphene superlattice with period l formed by position-dependent gap and band shift. As was shown in Ref.11, such structure can be realized, e.g., on the base of graphene deposited on a strip substrate combined from silicon oxide and *h*-BN (Fig.1). The SL electronic structure in the vicinity of \mathbf{K} -point of the Brillouin zone is described by the Dirac-like Hamiltonian

$$\hat{H} = v_F \hat{\mathbf{p}} \hat{\boldsymbol{\sigma}} + V(x) \hat{1} + \Delta(x) \hat{\sigma}_z \quad (1)$$

where $\hat{\mathbf{p}}$ is the momentum operator, $\hat{\sigma}_i$ are the Pauli matrices, $\hat{1}$ is a unit 2×2 matrix, $v_F \approx 10^8$ cm/s is the Fermi velocity, and $\Delta(x)$, $V(x)$ are periodic functions equal to Δ and V , respectively, at $a \leq x \leq l$, and zero at $0 \leq x < a$. Here, the potential V defines the shift of the forbidden band center in the gapped graphene with respect to the Dirac point in the gapless graphene^{11,12} (see Fig.1).

The Dirac equation

$$\hat{H} \Psi(x, y) = E \Psi(x, y) \quad (2)$$

admits the solutions of the form $\Psi(x, y) = \exp(ik_y y) \Psi(x)$, where the two-component spinor envelope function $\Psi(x)$ satisfies the equation

$$i \frac{d\Psi}{dx} = \hat{h}(x) \Psi(x) \quad (3)$$

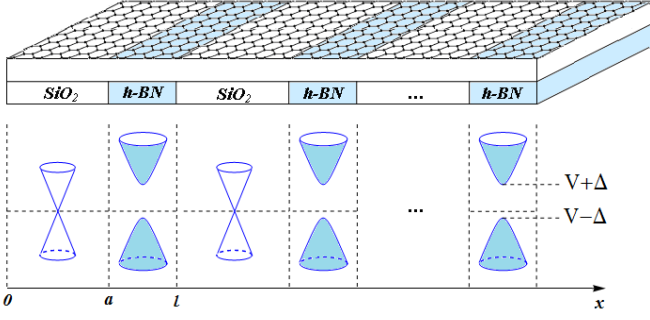


FIG. 1: (Color online) Top: graphene layer on the striped substrate composed of silicon oxide and hexagonal boron nitride. Bottom: schematic diagram showing the electronic energy spectrum in graphene SL.

with

$$\hat{h}(x) = \begin{pmatrix} ik_y & \frac{V(x)-E-\Delta(x)}{\hbar v_F} \\ \frac{V(x)-E+\Delta(x)}{\hbar v_F} & -ik_y \end{pmatrix}. \quad (4)$$

The formal solution of Eq.(3) is

$$\Psi(x) = \hat{\mathcal{R}}_x \exp\left(-i \int_{x_0}^x \hat{h}(x_1) dx_1\right) \Psi(x_0), \quad (5)$$

where $\hat{\mathcal{R}}_x$ is the spatial ordering operator.^{13,14} This expression can be simplified as

$$\Psi(x) = \exp(-i(x-x_0)\hat{h})\Psi(x_0) \quad (6)$$

if both points x and x_0 belong to the space-homogeneous region.

It is convenient to define the matrix

$$\hat{t}(x-x_0) = \exp(-i(x-x_0)\hat{h}). \quad (7)$$

Then $\Psi(l) = \hat{t}(l-a)\hat{t}(a)\Psi(0) = \hat{T}\Psi(0)$. Performing the ordinary expansion of exponential function in power series and using Eq.(4) one gets:

$$\hat{t}(x-x_0) = \begin{pmatrix} \cos \alpha + \frac{k_y}{K(x)} \sin \alpha & -i \sin \alpha \frac{V(x)-E-\Delta(x)}{\hbar v_F K(x)} \\ -i \sin \alpha \frac{V(x)-E+\Delta(x)}{\hbar v_F K(x)} & \cos \alpha - \frac{k_y}{K(x)} \sin \alpha \end{pmatrix}, \quad (8)$$

where $K(x) = \sqrt{((V(x)-E)^2 - \Delta^2(x))/(\hbar v_F)^2 - k_y^2}$, $\alpha = (x-x_0)K(x)$. Note, that $\det(t) = 1$ and, consequently $\det(T) = 1$ as well. This equality and the Bloch condition $\Psi(l) = \Psi(0) \exp(ikl)$ (here, k is the Bloch wave vector) yield the dispersion relation $2 \cos(kl) = \text{Tr}(T)$ for the 1D graphene-based SL. Using Eq.(8) one can find $\text{Tr}(T) = \text{Tr}(t(l-a)t(a))$. Accordingly, the resulting dispersion equation reads

$$\cos(kl) = \cos(k_x a) \cos(q_x(l-a)) + \frac{EV - (\hbar v_F k_x)^2}{(\hbar v_F)^2 k_x q_x} \sin(k_x a) \sin(q_x(l-a)), \quad (9)$$

with $k_x \equiv K(+0)$, $q_x \equiv K(l-0)$. At $(V-E)^2 - \Delta^2 < (\hbar v_F k_y)^2$, the wave number q_x is imaginary and the allowed energies are given by Eq.(9) with q_x replaced by $i|q_x|$.

Eq.(9) for the allowed energies was obtained also in Ref.11 via wave function matching. However some results of this work concerning the miniband structure and existence of the interface states seem questionable. Below we discuss these issues in detail. Note that at $\Delta = 0$, Eq.(9) coincides with the one found for single-layer graphene in a periodic piecewise constant potential $V(x)$.¹⁴⁻¹⁶

III. ELECTRONIC STRUCTURE

The SL band structure depends on the system parameters as well as on the y -component of the wave vector. As seen from the Eq.(9), the dispersion relation is invariant with respect to the simultaneous replacements $E \rightarrow -E$, $V \rightarrow -V$. Therefore, in what follows we shall consider, for definiteness, only nonnegative values of the relative band shift: $V \geq 0$. When $V = 0$, the energy spectrum is completely symmetric related to the value $E = 0$ corresponding to the original Dirac point in the gapless graphene. In this case the two first minibands symmetrically situated above and below the original Dirac point are the conduction and valence ones, respectively. As V increases, the conduction and valence minibands gradually shift up. Below we shall concentrate on these two minibands only, assuming the Fermi level to be in between (or, at least, within one of the minibands) at any V .

The electron and hole energies as functions of k at $k_y = 0$, $\Delta = 26.5$ meV and for different values of the potential V and for different widths a are plotted in Fig.2. The parameters we choose are appropriate for graphene. Dots and dashed (red) line correspond to $V = 0$ and $V = 24.2$ meV, respectively and $a = l/2$. It is seen that when V becomes nonzero, the electron band turns out to be narrower than the hole one. The electron and hole energies for $a = l/6$, $V = 24.2$ meV are shown with solid (blue) line. We can see that, as the gapped graphene fraction in the SL increases, the electron-hole minigap increases too. Nevertheless, in any case, at $k_y = 0$ the minigap cannot exceed the gap value 2Δ .¹⁷ Indeed, it is clear that if the whole graphene layer is gapped, i.e. $a = 0$, the forbidden miniband should be 2Δ (at $k_y=0$).

Figure 3 illustrates the dependence of the electron and hole energies on k_y at different V and Δ , and $k = 0$, $a = l/2$, $l = 60$ nm. We show only semiaxis $k_y > 0$ because of the symmetry $k_y \rightarrow -k_y$ in the dispersion law (9). The energies in the figure are counted from the minigap center (whose position determining at $k = k_y = 0$ depends on V) for $V = 24.2$ meV (short-dashed line) and $V = 110$ meV (long-dashed line) at $\Delta = 26.5$ meV. In other cases the energy origin coincides with the contact-point energy. Our calculations demonstrate a monotonous expansion of the forbidden miniband with $|k_y|$ increasing (short- and

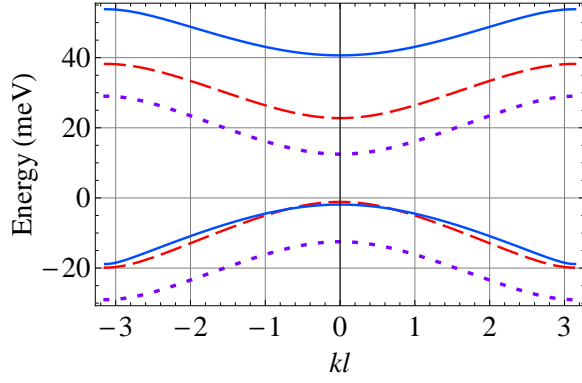


FIG. 2: (Color online) Two low-energy minibands of the SL spectrum with $k_y = 0$, $l = 60$ nm, and $\Delta = 26.5$ meV. The dotted (violet) line corresponds to the barrier height $V = 0$ and $a = l/2$. The solid (blue) and dashed (red) lines correspond to the width of gapless graphene $a = l/6$ and $a = l/2$ respectively; $V \simeq 24.2$ meV in both cases.

long-dashed (blue) lines in Fig.3) until V becomes greater than some threshold value V_c (for chosen set of parameters $V_c = 143.26$ meV). When $V = V_c$ (thick solid line in Fig.3), the electron and hole energy branches touch each other at $k = k_y = 0$ closing the minigap. When V exceeds V_c , the minigap at $k = k_y = 0$ opens, but two extra Dirac points appear in symmetric positions on the k_y -axis (thin solid line in Fig.3), and never then vanish. Thus, beginning with $V = V_c$ the gap-induced SL becomes gapless. Further increase of V results in appearance of new additional Dirac points, which originate from $k_y = 0$ at certain values of the potential V (see below).

Such a behavior is not unique. As was shown in Refs 18-20 for gapless graphene, the new Dirac points can emerge in the presence of a sinusoidal or squarewell SL potential. A simple analytical expression for the location of these points in \mathbf{k} -space has been obtained by different research groups.^{14,16}

It is clearly seen from Fig.3 that extra Dirac point located at $k_y l \simeq 6.3$ for $\Delta = 0$ (dots) remains also in the case where the SL consists of both gapless and gapped graphene. However, the position of the Dirac point in this case slightly shifts towards zero. To find the location of the Dirac points in \mathbf{k} -space we note that $k_x(E, k_y)$ and $q_x(E, k_y)$ coincide at

$$E_0(V) = \frac{V^2 - \Delta^2}{2V}. \quad (10)$$

Correspondingly, Eq.(9) at $a = l/2$, $k = 0$ and $E = E_0$ turns into

$$1 = \cos^2 \frac{k_x l}{2} + \frac{E_0 V - E_0^2 + \hbar^2 v_F^2 k_y^2}{(\hbar v_F k_x)^2} \sin^2 \frac{k_x l}{2}. \quad (11)$$

Obviously this equation is satisfied if $k_x l = 2\pi n$ ($n \neq 0$), which leads to

$$k_y l = \sqrt{\left(\frac{E_0 l}{\hbar v_F}\right)^2 - (2\pi n)^2}, \quad (12)$$

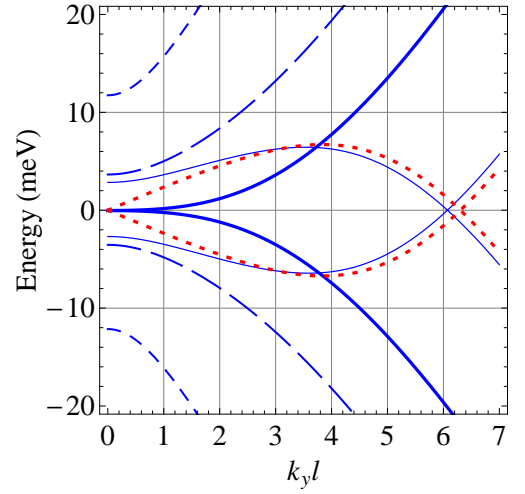


FIG. 3: (Color online) k_y -dependence of the electron energies in the conduction and valence minibands at $k = 0$, $l = 60$ nm, $a = l/2$, $\Delta = 0$, and $V = 196$ meV (dots (red)). For other curves $\Delta = 26.5$ meV and $V = 24.2$ meV (short-dashed line); $V = 110$ meV (long-dashed line); $V = 143.26$ meV (thick solid line), and $V = 196$ meV (thin solid line). The zeroth energy corresponds to the minigap center for the dashed lines, and to the contact points for all the others.

where n is integer.

One can check that for $a = l/2$, the right side of Eq.(9) has local maximum (equal to unity) at $E = E_0$ and k_y defined by Eq.(12). This means coincidence of conduction and valence miniband edges.

According to Eq.(12), in general case, when the ratio $E_0 l / 2\pi \hbar v_F$ is not integer, the number of Dirac points N_D symmetrically situated around $k_y = 0$ is given by

$$N_D = 2 \left\lfloor \frac{E_0 l}{2\pi \hbar v_F} \right\rfloor, \quad (13)$$

where $\lfloor \dots \rfloor$ denotes an integer part. One of the contact points is always located at $k_y = 0$ if $E_0 l / \hbar v_F = 2\pi j$ ($j = 1, 2, \dots$). In this case the total number of Dirac points is odd: $N_D = 2j - 1$, and the dispersion along k_y -axis is almost flat in the vicinity of the Dirac point situated at $k_y = 0$: $E - E_0 \sim \pm k_y^2 \Delta / n^2$. Similar behavior of the dispersion curves takes place in SL based on a gapless graphene,¹⁶ where, however, dispersion is defined by the third power of the y -component of the wave vector: $E - E_0 \sim \pm k_y^3 \Delta / n^2$. Note that, the coefficient before k_y^2 in our case is proportional to Δ only if $\Delta \ll 2\pi \hbar v_F / l$. In other case, its dependence on Δ becomes more complex.

Thus, now we can write analytically the inequality for the system parameters corresponding to the formation of the gapless SL. Evidently, the gap separating the conduction and valence minibands vanishes if

$$\frac{(V^2 - \Delta^2)l}{4\pi \hbar v_F V} \geq 1. \quad (14)$$

The case of the rigorous equality in Eq.(14) corresponds

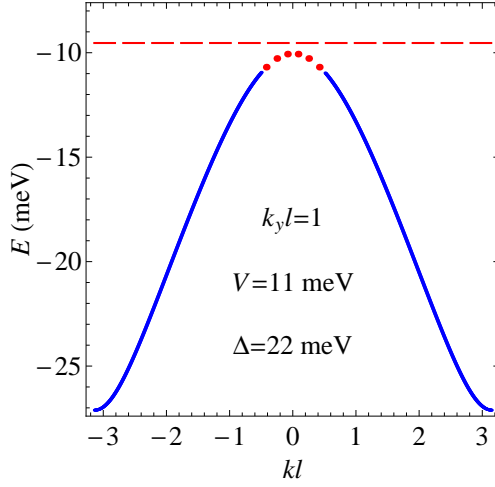


FIG. 4: (Color online) Hole band of the spectrum of SL for $a = l/2$, $l = 60$ nm. Top of the energy band depicted by the dots (red) corresponds to interface states. Dashed (red) line shows the interface energy level for an isolated heterojunction.

to the threshold value of the potential: $V = V_c$ (the positive root of the quadratic equation).

We do not discuss here the case $a \neq l/2$. We expect that Dirac points appear in this case too. However, the electron-hole miniband profile should be significantly asymmetric related to the Fermi level similarly to that takes place in SL based on a gapless graphene.¹⁶

IV. INTERFACE STATES

As was shown by Ratnikov and Silin²¹ interface states (ISs) can exist in graphene-based heterojunctions. It was found that ISs result from the crossing of dispersion curves of gapless and gapped graphene modifications. However, the author of Ref.11 stated that appearance of IS minibands is impossible in a graphene-based superlattice. In contrast to this conclusion we found that the ISs can arise under certain conditions discussed below. Since the wave functions of these states behave as exponentials along x -axis, the wave vectors k_x and q_x should be imaginary, so that

$$(\hbar v_F k_y)^2 > E^2, \quad (\hbar v_F k_y)^2 + \Delta^2 > (E - V)^2. \quad (15)$$

In this case Eq.(9) transforms into

$$\cos(kl) = \cosh(k'_x a) \cosh(q'_x (l - a)) + \frac{EV - E^2 + (\hbar v_F k_y)^2}{(\hbar v_F)^2 k'_x q'_x} \sinh(k'_x a) \sinh(q'_x (l - a)), \quad (16)$$

with $k'_x = \sqrt{k_y^2 - \frac{E^2}{(\hbar v_F)^2}}$, $q'_x = \sqrt{k_y^2 + \frac{\Delta^2 - (V - E)^2}{(\hbar v_F)^2}}$.

Evidently the solution of this equation can exist only if

$$(\hbar v_F k_y)^2 - E^2 < -EV. \quad (17)$$

Since the left side of this expression is positive (see Eq.(15)) the allowed values of the energy should be negative if $V > 0$ and *vice versa*. It is not difficult to show that the inequalities (15) and (17) have the solutions when Δ and V differ from zero, $\Delta > |V|$, and $k_y^2 < k_c^2$, where $k_c^2 = \Delta^2(\Delta^2 - V^2)/(\hbar v_F V)^2$.

In Fig.4 the hole miniband of the SL with $a = l/2$, $l = 60$ nm is plotted for $V = 11$ meV, $\Delta = 22$ meV, and $k_y l = 1$. Upper narrow slice of the valence miniband depicted by dots is formed by the interface states. Indeed, it is possible to verify that any energy value from this range obey the inequalities (15) and (17) for the above parameters. Dashed (red) line in the figure shows the interface energy level $|E| = \hbar v_F |k_y| (1 - V^2/\Delta^2)^{1/2}$ for an isolated heterojunction.¹⁷

V. CONCLUDING REMARKS

We have considered the simple model of a one-dimensional SL in which the gap and potential profile are piecewise constant functions. In the framework of this model the dispersion relation for Dirac electrons was obtained, and the structure of low-energy minibands was investigated depending on the potential V and other parameters of the SL.

It was found that if V becomes greater than some critical value V_c , the electron-hole minigap turns out to be an essentially non-monotonous function of the y -component of the electron wave vector. In particular, when $V > V_c$ the forbidden miniband turns into zero at some values of k_y , and new Dirac points arise symmetrically relatively to $k_y = 0$ in the electronic spectrum. As a result, the SL becomes gapless. Appearance of new Dirac points at $k_y \neq 0$ is typical as well for SL induced by the potential modulation of a gapless graphene.^{14,16,18-20} Thus, one may conclude that such a reconstruction of the electron spectrum in a certain extent represents a universal property of graphene-based superlattices. In the case where the widths of the gapless and gapped graphene strips in the SL are equal, we found the positions of the Dirac points in \mathbf{k} -space and obtained the expression for the threshold value V_c of the potential responsible for their appearance.

Finally, we found that the interface states can exist in the gap-induced SL at certain conditions.

VI. ACKNOWLEDGMENTS

This work was supported by the Russian Foundation for Basic Research (Grant No. 11-02-00960a) and Russian Ministry of Education and Science (Contract No. 07.514.11.4147).

-
- ¹ A.H.Castro Neto, F.Guinea, N.M.R.Peres, K.S.Novoselov, and A.K.Geim, *Rev. Mod. Phys.* **81**, 109 (2009).
 - ² O.Klein, *Z. Phys.* **53**, 157 (1929).
 - ³ M.I.Katsnelson, K.S.Novoselov, and A.K.Geim, *Nature Phys.* **2**, 620 (2006).
 - ⁴ G.M.Maksimova, V.Ya.Demikhovskii, and E.V.Frolova, *Phys. Rev. B* **78**, 235321 (2008); T.M.Rusin and W.Zawadzki, *Phys. Rev. B* **80**, 045416 (2009).
 - ⁵ A.K.Geim and K.S.Novoselov, *Nat. Matter* **6**, 183 (2007).
 - ⁶ A. De Martino, L. Dell Anna, and R.Egger, *Phys. Rev. Lett.* **98**, 066802 (2007).
 - ⁷ G.Giovannetti, P.A.Khomyakov, G.Brocks, P.J.Kelly, and J. van den Brink, *Phys. Rev. B* **76**, 073103 (2007).
 - ⁸ S.Lebegue, M.Klintenberg, O.Eriksson, and M.I.Katsnelson, *Phys. Rev. B* **79**, 245117 (2009).
 - ⁹ N.M.R.Peres, *J. Phys.: Condens. Matter* **21**, 095501 (2009).
 - ¹⁰ G.Giavaras and F.Nori, *Appl. Phys. Lett.* **97**, 243106 (2010).
 - ¹¹ P.V.Ratnikov, *JETP Lett.* **90**, 469 (2009).
 - ¹² P.V.Ratnikov and A.P.Silin, *JETP* **114**, 512 (2012).
 - ¹³ B.H.J.McKellar and G.J.Stephenson, *Phys. Rev. A* **36**, 2566 (1987).
 - ¹⁴ D.P.Arovas, L.Brey, H.A.Fertig, Eun-Ah Kim, and K.Zeigler, *New Journal of Physics* **12**, 123020 (2010).
 - ¹⁵ M.Barbier, F.M.Peeters, P.Vasilopoulos, and J.M.Pereira, *Phys. Rev. B* **77**, 115446 (2008).
 - ¹⁶ M.Barbier, P.Vasilopoulos, and F.M.Peeters, *Phys. Rev. B* **81**, 075438 (2010).
 - ¹⁷ The author of Ref.11 assert that the forbidden band width can several times exceed the gap value 2Δ .
 - ¹⁸ J.H.Ho, Y.H.Chiu, S.J.Tsai, and M.F.Lin, *Phys. Rev. B* **79**, 115427 (2009).
 - ¹⁹ C-H.Park, Y-W.Son, L.Yang, M.L.Cohen, and S.G.Louie, *Phys. Rev. Lett.* **103**, 046808 (2009).
 - ²⁰ L.Brey and H.A.Fertig, *Phys. Rev. Lett.* **103**, 046809 (2009).
 - ²¹ P.V.Ratnikov and A.P.Silin, *Physics of the Solid State* **52**, 1763 (2010).